Search for High-Mass e+e- Resonances in pp-bar Collisions at sqrt[s]=1.96 TeV

Massachusetts Institute of Technology

Search for High-Mass e^+e^- Resonances in $p\bar{p}$ Collisions at $\sqrt{s} = 1.96$ TeV

T. Aaltonen,[24] J. Adelman,[14] T. Akimoto,[56] M. G. Albrow,[18] B. Álvarez González,[12] S. Amerio,[44a,44b] D. Amidei,[35]
A. Anastassov,[39] A. Annovi,[20] J. Antos,[15] G. Apollinari,[18] A. Apresyan,[49] T. Arisawa,[58] A. Artikov,[16] W. Ashmanskas,[18]
A. Attal,[4] A. Aurisano,[54] F. Azfar,[43] P. Azzurri,[47a,47d] W. Badgett,[18] A. Barbaro-Galtieri,[29] V. E. Barnes,[49] B. A. Barnett,[26]
V. Bartsch,[31] G. Bauer,[33] P.-H. Beauchemin,[34] F. Bedeschi,[47a] D. Beecher,[31] S. Behari,[26] G. Bellettini,[47a,47b] J. Bellinger,[60]
D. Benjamin,[17] A. Beretvas,[18] J. Beringer,[29] A. Bhatti,[51] M. Binkley,[18] D. Bisello,[44a,44b] I. Bizjak,[31,w] R. E. Blair,[2]
C. Blocker,[7] B. Blumenfeld,[26] A. Bocci,[17] A. Bodek,[50] V. Boisvert,[50] G. Bolla,[49] D. Bortoletto,[49] J. Boudreau,[48]
A. Boveia,[11] B. Brau,[11,b] A. Bridgeman,[25] L. Brigliadori,[44a] C. Bromberg,[36] E. Brubaker,[14] J. Budagov,[16] H. S. Budd,[50]
S. Budd,[25] S. Burke,[18] K. Burkett,[18] G. Busetto,[44a,44b] P. Bussey,[22] A. Buzatu,[34] K. L. Byrum,[2] S. Cabrera,[17,u]
C. Calancha,[32] M. Campanelli,[36] M. Campbell,[35] F. Canelli,[18] A. Canepa,[46] B. Carls,[25] D. Carlsmith,[60] R. Carosi,[47a]
S. Carrillo,[19,m] S. Carron,[34] B. Casal,[12] M. Casarsa,[18] A. Castro,[6a,6b] P. Catastini,[47a,47c] D. Cauz,[55a,55b] V. Cavaliere,[47a,47c]
M. Cavalli-Sforza,[4] A. Cerri,[29] L. Cerrito,[31,n] S. H. Chang,[28] Y. C. Chen,[1] M. Chertok,[8] G. Chiarelli,[47a] G. Chlachidze,[18]
F. Chlebana,[18] K. Cho,[28] D. Chokheli,[16] J. P. Chou,[23] G. Choudalakis,[33] S. H. Chuang,[53] K. Chung,[13] W. H. Chung,[60]
Y. S. Chung,[50] T. Chwalek,[50] C. I. Ciobanu,[27] M. A. Ciocci,[45] A. Clark,[47a,47c] D. Clark,[7] G. Compostella,[44a]
M. E. Convery,[18] J. Conway,[8] M. Cordelli,[20] G. Cortiana,[44a,44b] C. A. Cox,[8] D. J. Cox,[8] F. Crescioli,[47a,47b]
C. Cuenca Almenar,[8,u] J. Cuevas,[12,r] R. Culbertson,[18] J. C. Cully,[35] D. Dagenhart,[18] M. Datta,[18] T. Davies,[22]
P. de Barbaro,[50] S. De Cecco,[52a] A. Deisher,[29] G. De Lorenzo,[4] M. Dell'Orso,[47a,47b] C. Deluca,[4] L. Demortier,[51] J. Deng,[17]
M. Deninno,[6a] P. F. Derwent,[18] G. P. di Giovanni,[45] C. Dionisi,[52a,52b] B. Di Ruzza,[55a,55b] J. R. Dittmann,[5] M. D'Onofrio,[4]
S. Donati,[47a,47b] P. Dong,[9] J. Donini,[44a] T. Dorigo,[44a] S. Dube,[53] J. Efron,[40] A. Elagin,[54] R. Erbacher,[8] D. Errede,[25]
S. Errede,[25] R. Eusebi,[18] H. C. Fang,[29] S. Farrington,[43] W. T. Fedorko,[14] R. G. Feild,[61] M. Feindt,[27] J. P. Fernandez,[32]
C. Ferrazza,[47a,47d] R. Field,[19] G. Flanagan,[49] R. Forrest,[8] M. J. Frank,[5] M. Franklin,[23] J. C. Freeman,[18] I. Furic,[19]
M. Gallinaro,[52a] J. Galyardt,[13] F. Garberson,[11] J. E. Garcia,[21] A. F. Garfinkel,[49] K. Genser,[18] H. Gerberich,[25] D. Gerdes,[35]
A. Gessler,[27] S. Giagu,[52a,52b] V. Giakoumopoulou,[3] P. Giannetti,[47a] K. Gibson,[48] J. L. Gimmell,[50] C. M. Ginsburg,[18]
N. Giokaris,[3] M. Giordani,[55a,55b] P. Giromini,[20] M. Giunta,[47a,47b] G. Giurgiu,[26] V. Glagolev,[16] D. Glenzinski,[18] M. Gold,[38]
N. Goldschmidt,[19] A. Golossanov,[18] G. Gomez,[12] G. Gomez-Ceballos,[33] M. Goncharov,[54] O. González,[32] I. Gorelov,[38]
A. T. Goshaw,[17] K. Goulianos,[51] A. Gresele,[44a,44b] S. Grinstein,[23] C. Grosso-Pilcher,[14] R. C. Group,[18] U. Grundler,[25]
J. Guimaraes da Costa,[23] Z. Gunay-Unalan,[36] C. Haber,[29] K. Hahn,[33] S. R. Hahn,[18] E. Halkiadakis,[53] B.-Y. Han,[50]
J. Y. Han,[50] F. Happacher,[20] K. Hara,[56] D. Hare,[53] M. Hare,[57] S. Harper,[43] R. F. Harr,[59] R. M. Harris,[18] M. Hartz,[48]
K. Hatakeyama,[51] C. Hays,[43] M. Heck,[27] A. Heijboer,[46] J. Heinrich,[46] C. Henderson,[33] M. Herndon,[60] J. Heuser,[27]
S. Hewamanage,[5] D. Hidas,[17] C. S. Hill,[11,d] D. Hirschbuehl,[27] A. Hocker,[18] S. Hou,[1] M. Houlden,[30] S.-C. Hsu,[29]
B. T. Huffman,[43] R. E. Hughes,[40] U. Husemann,[61] J. Huston,[36] J. Incandela,[11] G. Introzzi,[47a] M. Iori,[52a,52b] A. Ivanov,[8]
E. James,[18] B. Jayatilaka,[17] E. J. Jeon,[28] M. K. Jha,[6a] S. Jindariani,[18] W. Johnson,[8] M. Jones,[49] K. K. Joo,[28] S. Y. Jun,[13]
J. E. Jung,[28] T. R. Junk,[18] T. Kamon,[54] D. Kar,[19] P. E. Karchin,[59] Y. Kato,[42] R. Kephart,[18] J. Keung,[46] V. Khotilovich,[54]
B. Kilminster,[18] D. H. Kim,[62] H. S. Kim,[28] H. W. Kim,[28] J. E. Kim,[28] M. J. Kim,[20] S. B. Kim,[28] S. H. Kim,[56] Y. K. Kim,[14]
N. Kimura,[56] L. Kirsch,[7] S. Klimenko,[19] B. Knuteson,[33] B. R. Ko,[17] K. Kondo,[58] D. J. Kong,[28] J. Konigsberg,[19]
A. Korytov,[19] A. V. Kotwal,[17] M. Kreps,[27] J. Kroll,[46] D. Krop,[14] N. Krumnack,[5] M. Kruse,[17] V. Krutelyov,[11] T. Kubo,[56]
T. Kuhr,[27] N. P. Kulkarni,[59] M. Kurata,[56] Y. Kusakabe,[58] S. Kwang,[14] A. T. Laasanen,[49] S. Lami,[47a] S. Lammel,[18]
M. Lancaster,[31] R. L. Lander,[8] K. Lannon,[40,q] A. Lath,[53] G. Latino,[47a,47c] I. Lazzizzera,[44a,44b] T. LeCompte,[2] E. Lee,[54]
H. S. Lee,[14] S. W. Lee,[54,t] S. Leone,[47a] J. D. Lewis,[18] C.-S. Lin,[29] J. Linacre,[43] M. Lindgren,[18] E. Lipeles,[46] A. Lister,[8]
D. O. Litvintsev,[18] C. Liu,[48] T. Liu,[18] N. S. Lockyer,[46] A. Loginov,[61] M. Loreti,[44a,44b] L. Lovas,[15] D. Lucchesi,[44a,44b]
C. Luci,[52a,55b] J. Lueck,[27] P. Lujan,[29] P. Lukens,[18] G. Lungu,[51] L. Lyons,[43] J. Lys,[29] R. Lysak,[15] D. MacQueen,[34]
R. Madrak,[18] K. Maeshima,[18] K. Makhoul,[33] T. Maki,[24] P. Maksimovic,[26] S. Malde,[43] S. Malik,[31] G. Manca,[30,f]
A. Manousakis-Katsikakis,[3] F. Margaroli,[49] C. Marino,[27] C. P. Marino,[25] A. Martin,[61] V. Martin,[22,l] M. Martínez,[4]
R. Martínez-Ballarín,[32] T. Maruyama,[56] P. Mastrandrea,[52a] T. Masubuchi,[56] M. Mathis,[26] M. E. Mattson,[59] P. Mazzanti,[6a]
K. S. McFarland,[50] P. McIntyre,[54] R. McNulty,[30,k] A. Mehta,[30] P. Mehtala,[24] A. Menzione,[47a] P. Merkel,[49] C. Mesropian,[51]
T. Miao,[18] N. Miladinovic,[7] R. Miller,[36] C. Mills,[23] M. Milnik,[27] A. Mitra,[1] G. Mitselmakher,[19] H. Miyake,[56] N. Moggi,[6a]
C. S. Moon,[28] R. Moore,[18] M. J. Morello,[47a,47b] J. Morlok,[27] P. Movilla Fernandez,[18] J. Mülmenstädt,[29] A. Mukherjee,[18]
Th. Muller,[27] R. Mumford,[26] P. Murat,[18] M. Mussini,[6a,6b] J. Nachtman,[18] Y. Nagai,[56] A. Nagano,[56] J. Naganoma,[56]
K. Nakamura,[56] I. Nakano,[41] A. Napier,[57] V. Necula,[17] J. Nett,[60] C. Neu,[46,v] M. S. Neubauer,[25] S. Neubauer,[27]

J. Nielsen,[29,h] L. Nodulman,[2] M. Norman,[10] O. Norniella,[25] E. Nurse,[31] L. Oakes,[43] S. H. Oh,[17] Y. D. Oh,[28] I. Oksuzian,[19] T. Okusawa,[42] R. Orava,[24] S. Pagan Griso,[44a,44b] E. Palencia,[18] V. Papadimitriou,[18] A. Papaikonomou,[27] A. A. Paramonov,[14] B. Parks,[40] S. Pashapour,[34] J. Patrick,[18] G. Pauletta,[55a,55b] M. Paulini,[13] C. Paus,[33] T. Peiffer,[27] D. E. Pellett,[8] A. Penzo,[55a] T. J. Phillips,[17] G. Piacentino,[47a] E. Pianori,[46] L. Pinera,[19] K. Pitts,[25] C. Plager,[9] L. Pondrom,[60] O. Poukhov,[16,a] N. Pounder,[43] F. Prakoshyn,[16] A. Pronko,[18] J. Proudfoot,[2] F. Ptohos,[18,j] E. Pueschel,[13] G. Punzi,[47a,47b] J. Pursley,[60] J. Rademacker,[43,d] A. Rahaman,[48] V. Ramakrishnan,[60] N. Ranjan,[49] I. Redondo,[32] V. Rekovic,[38] P. Renton,[43] M. Renz,[27] M. Rescigno,[52a] S. Richter,[27] F. Rimondi,[6a,6b] L. Ristori,[47a] A. Robson,[22] T. Rodrigo,[12] T. Rodriguez,[46] E. Rogers,[25] S. Rolli,[57] R. Roser,[18] M. Rossi,[55a] R. Rossin,[11] P. Roy,[34] A. Ruiz,[12] J. Russ,[13] V. Rusu,[18] A. Safonov,[54] W. K. Sakumoto,[50] O. Saltó,[4] L. Santi,[55a,55b] S. Sarkar,[52a,52b] L. Sartori,[47a] K. Sato,[18] A. Savoy-Navarro,[45] P. Schlabach,[18] A. Schmidt,[27] E. E. Schmidt,[18] M. A. Schmidt,[14] M. P. Schmidt,[61,a] M. Schmitt,[39] T. Schwarz,[8] L. Scodellaro,[12] A. Scribano,[47a,47c] F. Scuri,[47a] A. Sedov,[49] S. Seidel,[38] Y. Seiya,[42] A. Semenov,[16] L. Sexton-Kennedy,[18] F. Sforza,[47a] A. Sfyrla,[25] S. Z. Shalhout,[59] T. Shears,[30] P. F. Shepard,[48] M. Shimojima,[56,p] S. Shiraishi,[14] M. Shochet,[14] Y. Shon,[60] I. Shreyber,[37] A. Sidoti,[47a] P. Sinervo,[34] A. Sisakyan,[16] A. J. Slaughter,[18] J. Slaunwhite,[40] K. Sliwa,[57] J. R. Smith,[8] F. D. Snider,[18] R. Snihur,[34] A. Soha,[8] S. Somalwar,[53] V. Sorin,[36] J. Spalding,[18] T. Spreitzer,[34] P. Squillacioti,[47a,47c] M. Stanitzki,[61] R. St. Denis,[22] B. Stelzer,[9,s] O. Stelzer-Chilton,[17] D. Stentz,[39] J. Strologas,[38] G. L. Strycker,[35] D. Stuart,[11] J. S. Suh,[28] A. Sukhanov,[19] I. Suslov,[16] T. Suzuki,[56] A. Taffard,[25,g] R. Takashima,[41] Y. Takeuchi,[56] R. Tanaka,[41] M. Tecchio,[35] P. K. Teng,[1] K. Terashi,[51] J. Thom,[18,i] A. S. Thompson,[22] G. A. Thompson,[25] E. Thomson,[46] P. Tipton,[61] P. Ttito-Guzmán,[32] S. Tkaczyk,[18] D. Toback,[54] S. Tokar,[15] K. Tollefson,[36] T. Tomura,[56] D. Tonelli,[18] S. Torre,[20] D. Torretta,[18] P. Totaro,[55a,55b] S. Tourneur,[45] M. Trovato,[47a] S.-Y. Tsai,[1] Y. Tu,[46] N. Turini,[47a,47c] F. Ukegawa,[56] S. Vallecorsa,[21] N. van Remortel,[24,c] A. Varganov,[35] E. Vataga,[47a,47d] F. Vázquez,[19,m] G. Velev,[18] C. Vellidis,[3] V. Veszpremi,[49] M. Vidal,[32] R. Vidal,[18] I. Vila,[12] R. Vilar,[12] T. Vine,[31] M. Vogel,[38] I. Volobouev,[29,t] G. Volpi,[47a,47b] P. Wagner,[46] R. G. Wagner,[2] R. L. Wagner,[18] W. Wagner,[27] J. Wagner-Kuhr,[27] T. Wakisaka,[42] R. Wallny,[9] C. Wang,[17] S. M. Wang,[1] A. Warburton,[34] D. Waters,[31] M. Weinberger,[54] J. Weinelt,[27] W. C. Wester III,[18] B. Whitehouse,[57] D. Whiteson,[46,g] A. B. Wicklund,[2] E. Wicklund,[18] S. Wilbur,[14] G. Williams,[34] H. H. Williams,[46] P. Wilson,[18] B. L. Winer,[40] P. Wittich,[18,i] S. Wolbers,[18] C. Wolfe,[14] T. Wright,[35] X. Wu,[21] F. Würthwein,[10] S. M. Wynne,[30] S. Xie,[33] A. Yagil,[10] K. Yamamoto,[42] J. Yamaoka,[53] U. K. Yang,[14,o] Y. C. Yang,[28] W. M. Yao,[29] G. P. Yeh,[18] J. Yoh,[18] K. Yorita,[14] T. Yoshida,[42] G. B. Yu,[50] I. Yu,[28] S. S. Yu,[18] J. C. Yun,[18] L. Zanello,[52a,52b] A. Zanetti,[55a] X. Zhang,[25] Y. Zheng,[9,e] and S. Zucchelli[6a,6b]

(CDF Collaboration)

[1]*Institute of Physics, Academia Sinica, Taipei, Taiwan 11529, Republic of China*
[2]*Argonne National Laboratory, Argonne, Illinois 60439, USA*
[3]*University of Athens, 157 71 Athens, Greece*
[4]*Institut de Fisica d'Altes Energies, Universitat Autonoma de Barcelona, E-08193, Bellaterra (Barcelona), Spain*
[5]*Baylor University, Waco, Texas 76798, USA*
[6a]*Istituto Nazionale di Fisica Nucleare Bologna, I-40127 Bologna, Italy;*
[6b]*University of Bologna, I-40127 Bologna, Italy*
[7]*Brandeis University, Waltham, Massachusetts 02254, USA*
[8]*University of California, Davis, Davis, California 95616, USA*
[9]*University of California, Los Angeles, Los Angeles, California 90024, USA*
[10]*University of California, San Diego, La Jolla, California 92093, USA*
[11]*University of California, Santa Barbara, Santa Barbara, California 93106, USA*
[12]*Instituto de Fisica de Cantabria, CSIC-University of Cantabria, 39005 Santander, Spain*
[13]*Carnegie Mellon University, Pittsburgh, Pennsylvania 15213, USA*
[14]*Enrico Fermi Institute, University of Chicago, Chicago, Illinois 60637, USA*
[15]*Comenius University, 842 48 Bratislava, Slovakia; Institute of Experimental Physics, 040 01 Kosice, Slovakia*
[16]*Joint Institute for Nuclear Research, RU-141980 Dubna, Russia*
[17]*Duke University, Durham, North Carolina 27708, USA*
[18]*Fermi National Accelerator Laboratory, Batavia, Illinois 60510, USA*
[19]*University of Florida, Gainesville, Florida 32611, USA*
[20]*Laboratori Nazionali di Frascati, Istituto Nazionale di Fisica Nucleare, I-00044 Frascati, Italy*
[21]*University of Geneva, CH-1211 Geneva 4, Switzerland*
[22]*Glasgow University, Glasgow G12 8QQ, United Kingdom*
[23]*Harvard University, Cambridge, Massachusetts 02138, USA*

[24]Division of High Energy Physics, Department of Physics, University of Helsinki and Helsinki Institute of Physics,
FIN-00014, Helsinki, Finland

[25]University of Illinois, Urbana, Illinois 61801, USA

[26]The Johns Hopkins University, Baltimore, Maryland 21218, USA

[27]Institut für Experimentelle Kernphysik, Universität Karlsruhe, 76128 Karlsruhe, Germany

[28]Center for High Energy Physics: Kyungpook National University, Daegu 702-701, Korea;
Seoul National University, Seoul 151-742, Korea; Sungkyunkwan University, Suwon 440-746, Korea;
Korea Institute of Science and Technology Information, Daejeon, 305-806, Korea;
Chonnam National University, Gwangju, 500-757, Korea

[29]Ernest Orlando Lawrence Berkeley National Laboratory, Berkeley, California 94720, USA

[30]University of Liverpool, Liverpool L69 7ZE, United Kingdom

[31]University College London, London WC1E 6BT, United Kingdom

[32]Centro de Investigaciones Energeticas Medioambientales y Tecnologicas, E-28040 Madrid, Spain

[33]Massachusetts Institute of Technology, Cambridge, Massachusetts 02139, USA

[34]Institute of Particle Physics: McGill University, Montréal, Canada H3A 2T8;
and University of Toronto, Toronto, Canada M5S 1A7

[35]University of Michigan, Ann Arbor, Michigan 48109, USA

[36]Michigan State University, East Lansing, Michigan 48824, USA

[37]Institution for Theoretical and Experimental Physics, ITEP, Moscow 117259, Russia

[38]University of New Mexico, Albuquerque, New Mexico 87131, USA

[39]Northwestern University, Evanston, Illinois 60208, USA

[40]The Ohio State University, Columbus, Ohio 43210, USA

[41]Okayama University, Okayama 700-8530, Japan

[42]Osaka City University, Osaka 588, Japan

[43]University of Oxford, Oxford OX1 3RH, United Kingdom

[44a]Istituto Nazionale di Fisica Nucleare, Sezione di Padova-Trento, I-35131 Padova, Italy;

[44b]University of Padova, I-35131 Padova, Italy

[45]LPNHE, Universite Pierre et Marie Curie/IN2P3-CNRS, UMR7585, Paris, F-75252 France

[46]University of Pennsylvania, Philadelphia, Pennsylvania 19104, USA

[47a]Istituto Nazionale di Fisica Nucleare Pisa, I-56127 Pisa, Italy;

[47b]University of Pisa, I-56127 Pisa, Italy;

[47c]University of Siena I-56127 Pisa, Italy;

[47d]Scuola Normale Superiore, I-56127 Pisa, Italy

[48]University of Pittsburgh, Pittsburgh, Pennsylvania 15260, USA

[49]Purdue University, West Lafayette, Indiana 47907, USA

[50]University of Rochester, Rochester, New York 14627, USA

[51]The Rockefeller University, New York, New York 10021, USA

[52a]Istituto Nazionale di Fisica Nucleare, Sezione di Roma 1, I-00185 Roma, Italy;

[52b]Sapienza Università di Roma, I-00185 Roma, Italy

[53]Rutgers University, Piscataway, New Jersey 08855, USA

[54]Texas A&M University, College Station, Texas 77843, USA

[55a]Istituto Nazionale di Fisica Nucleare Trieste/Udine, Italy;

[55b]University of Trieste/Udine, Italy

[56]University of Tsukuba, Tsukuba, Ibaraki 305, Japan

[57]Tufts University, Medford, Massachusetts 02155, USA

[58]Waseda University, Tokyo 169, Japan

[59]Wayne State University, Detroit, Michigan 48201, USA

[60]University of Wisconsin, Madison, Wisconsin 53706, USA

[61]Yale University, New Haven, Connecticut 06520, USA

[62]Center for High Energy Physics: Kyungpook National University, Daegu 702-701, Korea;
Seoul National University, Seoul 151-742, Korea;
Sungkyunkwan University, Suwon 440-746, Korea;
Korea Institute of Science and Technology Information, Daejeon, 305-806, Korea;
Chonnam National University, Gwangju, 500-757, Korea

A search for high-mass resonances in the e^+e^- final state is presented based on 2.5 fb^{-1} of $\sqrt{s} =$ 1.96 TeV $p\bar{p}$ collision data from the CDF II detector at the Fermilab Tevatron. The largest excess over the standard model prediction is at an e^+e^- invariant mass of 240 GeV/c^2. The probability of observing such an excess arising from fluctuations in the standard model anywhere in the mass range of 150–1000 GeV/c^2 is 0.6% (equivalent to 2.5σ). We exclude the standard model coupling Z' and the

Randall-Sundrum graviton for $k/\bar{M}_{\mathrm{Pl}} = 0.1$ with masses below 963 and 848 GeV/c^2 at the 95% credibility level, respectively.

The charged lepton-antilepton pair signature, in particular e^+e^- and $\mu^+\mu^-$, has been a leading discovery channel for new particles such as the J/ψ and Υ mesons and the Z boson since they have cleaner experimental signatures and lower backgrounds than hadronic signatures.

Many models beyond the standard model (SM) predict the existence of new particles decaying to lepton-antilepton pairs. The E_6 Z's [1] and the Randall-Sundrum (RS) graviton [2] are examples of specific new particles decaying to a lepton-antilepton final state. The Z'_ψ, Z'_χ, Z'_η, Z'_I, Z'_{sec}, and Z'_N are chosen for testing the E_6 model. Assuming one extra dimension, we test the RS model in the $k/\bar{M}_{\mathrm{Pl}}$ range between 0.01 and 0.1 [3], where k is the curvature of the extra dimension and $\bar{M}_{\mathrm{Pl}}$ is the reduced effective Planck scale.

In recent publications, the CDF [4] and D0 [5] Collaborations set limits on these models with 1.3 and 1.0 fb^{-1} of integrated luminosity and limits on Z' with SM coupling and RS graviton for $k/\bar{M}_{\mathrm{Pl}} = 0.1$ are 923 and 900 GeV/c^2, respectively. Using a data set twice as large (2.5 fb^{-1}), this Letter describes a search for e^+e^- resonances in the invariant-mass range of 150–1000 GeV/c^2, and we set upper limits on $\sigma(p\bar{p} \to X)\mathcal{B}(X \to e^+e^-)$ at the 95% credibility level (C.L.) where X is a spin 1 or spin 2 particle. We also set lower mass bounds on the Z' with SM coupling, the Z's in the E_6 model, and the RS graviton.

This analysis is based on data collected with the CDF II detector [6]. The relevant components of the detector for this analysis are the tracking system and the calorimeters. The tracking system consists of a 96 layer drift chamber called the central outer tracker (COT), surrounding an eight-layer silicon tracker. Both are inside a 1.4 T solenoidal magnet. The COT covers the range of pseudorapidity $|\eta| < 1.1$ [7], and the silicon tracker covers $|\eta|$ up to 2.0. The electromagnetic (EM) and hadronic calorimeters, which are sandwiches of lead (EM) or iron (hadronic) absorber and plastic scintillator. They are outside the magnet, and are divided into a central calorimeter ($|\eta| < 1.1$) and two plug calorimeters ($1.1 < |\eta| < 3.6$). Both the central and the plug EM calorimeters have fine-grained shower profile detectors at EM shower maximum.

We use the same on-line event selection criteria (triggers) used in our previous report [4]. Off-line events are required to have two isolated electrons [8], one in the central EM calorimeter and the other one in either the central (CC) or the plug (CP) EM calorimeters. Only electrons with E_T [7] greater than 25 GeV and $|\eta| < 2$ are used in order to ensure 100% trigger efficiency and coverage by the the silicon tracker. Electrons in the central EM calorimeter are required to have a well-measured track

in the COT system pointing at an energy deposit in the calorimeter. For electrons in the plug EM calorimeter, the track association uses a calorimeter-seeded silicon-tracking algorithm [9]. An opposite-charge requirement is applied to electron-objects pairs detected in the central EM calorimeter. No such requirement is applied when one electron is detected in the plug, where η-dependent charge misidentification occurs. Events with both electrons in the plug EM calorimeter are not considered in this Letter since adding them gains little sensitivity.

The PYTHIA [10] Tune A [11] Monte Carlo event generator is used to model the expected signals and backgrounds unless otherwise stated. For spin 1 Z', SM-like couplings are assumed, and for spin 2 resonances, the RS graviton model with $k/\bar{M}_{\mathrm{Pl}} = 0.1$ is used. The total selection efficiencies of spin 1 particles vary from 27% to 38% and those of spin 2 particles vary from 28% to 32% as functions of the particle mass in the search range.

There are three sources of background. One is Drell-Yan production of e^+e^- pairs (DY), which is the dominant source of background and is irreducible. Another is dijets and $W + $ jets production (referred to as "QCD" background) where one or more jets is misidentified as electron. Other contributions include $Z/\gamma^* \to \tau^+\tau^-$, $t\bar{t}$, and diboson ($W\gamma$, WW, WZ, ZZ, $\gamma\gamma$) production that collectively are referred to as "other SM" backgrounds.

The simulated DY prediction is normalized to the data after subtracting other SM and QCD backgrounds in an invariant-mass window from 76 to 106 GeV/c^2 for CC events and from 81 to 101 GeV/c^2 for CP events to estimate the DY background. Different mass windows are used because the QCD background rate in CP events is higher than in CC events. We assign a 3.6% systematic uncertainty in the DY prediction to take into account the invariant-mass dependence of the k-factor [12] that is the difference between the leading and the next-to-next-to-leading order DY cross sections. The uncertainty in the DY prediction due to the choice of the parton distribution function set CTEQ6M [13] using the Hessian method [14] is 3.7%–6.4%–13% (200–600–1000 GeV/c^2) depending on the invariant mass.

The QCD background estimation is determined from the experimental data. The estimate is obtained using the probability for a jet to be misidentified as an electron [15]. We measure this probability with a jet-triggered data sample. We then apply the misidentification probability to each jet in events with one good electron candidate and one or more jets. To estimate the dijet background contribution, events with W or Z candidates are removed from the sample before applying the jet misidentification

probability (MP). Events with W candidates are identified with one good electron and a large missing transverse energy $\not{E}_T$ [16] and events with Z candidates are identified with two "loose electrons". To estimate the $W +$ jets background, events with Z candidates are removed and events with W candidates are retained. The dominant systematic uncertainty in the predicted QCD background is due to the 20% uncertainty in the jet MP, which is obtained from the variation in the MP measured in the different jet data samples.

Other SM contributions to the background are estimated with simulation samples [17]. These simulated samples are normalized to the product of the theoretical cross sections and the integrated luminosity. Figure 1 shows the observed e^+e^- invariant-mass spectrum from 2.5 fb^{-1} of data together with the expected backgrounds.

The systematic uncertainty for other SM backgrounds is dominated by the 6% uncertainty in the integrated luminosity measurement [18] and 8% uncertainty in the theoretical cross sections [19]. Other systematic sources are the uncertainty on the scale factor of electron identification efficiency that comes from the difference between data and simulated events (1.3% for CC and 2.3% for CP events), the energy scale (1.0%), and the energy resolution (0.6% for CC and 0.3% for CP events), which affects the shape of the e^+e^- invariant-mass distribution. The uncertainty on the acceptance due to parton-distribution-function uncertainties is evaluated using the same method that was used for the DY prediction, and found to be 1.9% for CC and 0.6% for CP events.
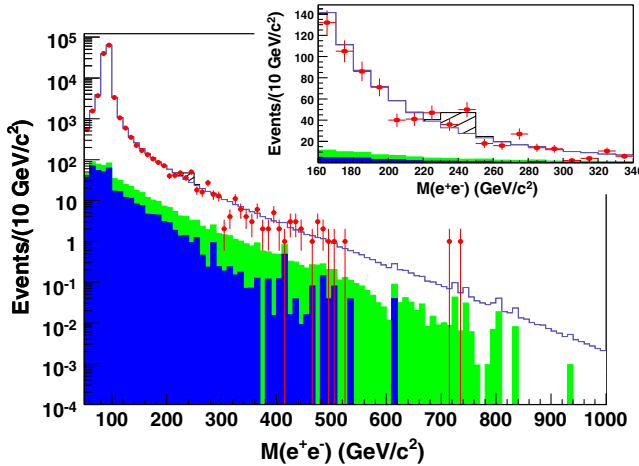

FIG. 1 (color online). Invariant-mass distribution of e^+e^- events compared to the expected backgrounds. Dots with error bars are data. The dark shaded region represents "other SM" background, the light shaded region shows QCD background, and the white region corresponds to $Z/\gamma^* \to e^+e^-$ background. The inset shows the same for the 240 GeV/c^2 region. The hatched histogram shows the shape of the expected signal from a 240 GeV/c^2 spin 1 particle (of negligible intrinsic width) on top of the total background. The hatched region is normalized to the number of excess events seen in the data.

The search for e^+e^- resonances in the high-mass range of 150–1000 GeV/c^2 uses an unbinned likelihood ratio statistic, λ, defined in Eqs. (1)–(3) [20]:

$$\lambda = \frac{\max\limits_{n_b \geq 0} \mathcal{L}_b}{\max\limits_{n_b \geq 0, n_s \geq 0} \mathcal{L}_{s+b}}, \quad 0 \leq \lambda \leq 1, \quad 0 \leq -2\ln\lambda \leq \infty, \tag{1}$$

$$\mathcal{L}_{s+b} = \frac{(n_s + n_b)^N e^{-(n_s + n_b)}}{N!} \prod_i^N \frac{n_s S(x_i|\mu) + n_b B(x_i)}{n_s + n_b}, \tag{2}$$

$$\mathcal{L}_b = \frac{n_b^N e^{-n_b}}{N!} \prod_i^N B(x_i), \tag{3}$$

where $\mathcal{L}_b$ is the likelihood for a null hypothesis that is described by the SM only, $\mathcal{L}_{s+b}$ is the likelihood for a test hypothesis that is described by physics beyond the SM together with the SM. The quantities n_s and n_b are the number of signal and background candidates which are determined by the fit and N is the number of candidates observed in data, each represented by a vector $\{x_i\}$ of observables. The signal probability density function (PDF), $S(x|\mu)$, is a Gaussian with a floating mean μ and a fixed width, and $B(x)$ is a background PDF obtained from the total background template. The widths of the signal PDF are determined from simulation ($\sigma_{M_{ee}} = 0.8565$ GeV/$c^2 + 0.0192 M_{ee}$ for $M_{ee} > 150$ GeV/c^2) with the assumption that the decay widths of resonances are much less than the experimental resolution. The quantities $\mathcal{L}_{s+b}$ and the $\mathcal{L}_b$ are maximized separately without external background constraints. The function $-2\ln\lambda$ is calculated over the search range of 150–1000 GeV/c^2 and the most prominent local maxima are listed in Table I. The most significant deviation between data and the SM prediction occurs at an invariant mass of 241.3 GeV/c^2 where $-2\ln\lambda$ is 14.4. The (data $-$ background)/σ_B [21] corresponding to the region of maximum $-2\ln\lambda$ is calculated by counting the number of observed events and estimated backgrounds within $\pm 2\sigma_{M_{ee}}$ of the maximum, and it is 3.8.

To estimate the probability of observing an excess equal to or greater than the maximum observed excess anywhere in the search range of 150–1000 GeV/c^2, we simulated 100 000 experiments assuming background only. The distribution of maximum $-2\ln\lambda$ on these simulated experiments is shown in Fig. 2. Assuming only SM physics, the probability of observing a number of events equal to or

TABLE I. The prominent local maxima in the search range of 150–1000 GeV/c^2.

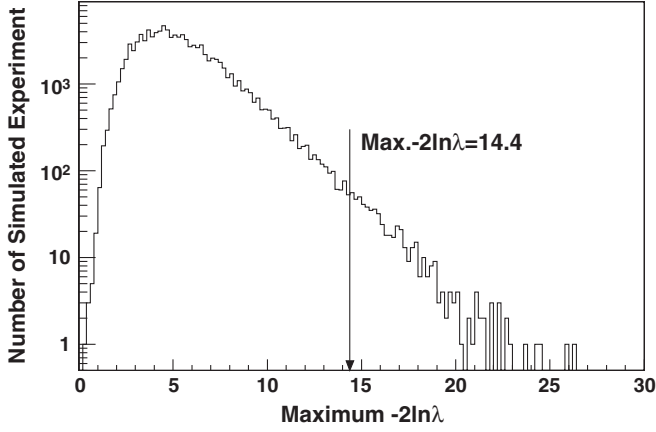| M_X (GeV/c^2)	241.3	272.7	478.9	725.2
$-2\ln\lambda$	14.4	3.7	2.6	4.1

FIG. 2.   Distribution of maximum $-2\ln\lambda$ in simulated experiments that assume only background. The arrow indicates the value observed in data: $-2\ln\lambda = 14.4$.

greater than the observed excess is defined as the fraction of simulated experiments with maximum $-2\ln\lambda$ equal to or greater than 14.4, and is 0.6% which corresponds to the 2.5σ level of excess over the background.
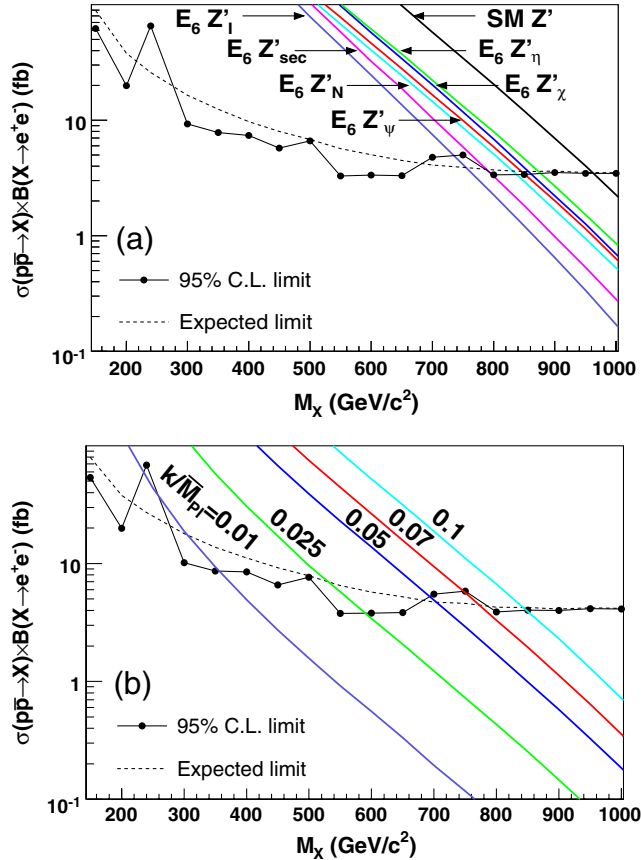

FIG. 3 (color online).   The upper limits on $\sigma(p\bar{p} \to X)\mathcal{B}(X \to e^{+}e^{-})$ as function of the mass of an X particle at the 95% C.L. where X is a spin 1 particle (a) or a spin 2 particle (b) together with model predictions.

TABLE II.   Expected and observed 95% C.L. lower limits on Z's masses.

Z' Model	Z'_{SM}	Z'_{ψ}	Z'_{χ}	Z'_{η}	Z'_{I}	Z'_{sec}	Z'_{N}
Expected Limit (GeV/c^2)	961	846	857	873	755	788	831
Observed Limit (GeV/c^2)	963	851	862	877	735	792	837

Upper limits on $\sigma(p\bar{p} \to X)\mathcal{B}(X \to e^{+}e^{-})$ at the 95% C.L. are calculated as a function of mass using a Bayesian binned likelihood method with a full consideration of uncertainties on the total signal efficiency and the background estimation [22]. Figure 3(a) shows the observed upper limits from data and the expected limits from background-only simulated events for spin 1 particles as a function of the $e^{+}e^{-}$ invariant mass, together with the expected cross sections for Z's [23]. Figure 3(b) shows the same but for spin 2 particles, together with the expected cross sections for RS gravitons. The cross sections for Z's and RS gravitons are calculated at leading order with PYTHIA and then multiplied by a factor of 1.3 in order to approximate a next-to-leading-order prediction as done in reports of earlier results. Table II shows the lower mass limits of the SM coupling and E_6 Z's and Fig. 4 shows the excluded RS graviton mass region with respect to $k/\bar{M}_{Pl}$.

To conclude, we have searched for $e^{+}e^{-}$ resonances with 2.5 fb^{-1} of data collected by the CDF II detector. The largest excess over the standard model prediction is at an $e^{+}e^{-}$ invariant mass of 240 GeV/c^2. The probability of observing such an excess arising from fluctuation in the standard model anywhere in the mass range of 150–1000 GeV/c^2 is 0.6%. We also set upper limits on $\sigma(p\bar{p} \to X)\mathcal{B}(X \to e^{+}e^{-})$ at the 95% C.L. for spin 1 and spin 2 particles. The SM coupling Z' with mass below 963 GeV/c^2 and the E_6 Z's with masses below 735/877 (lightest/heaviest) GeV/c^2 are excluded at the 95% C.L. RS gravitons with masses below 848 GeV/c^2 are excluded at the 95% C.L. for $k/\bar{M}_{Pl} = 0.1$.
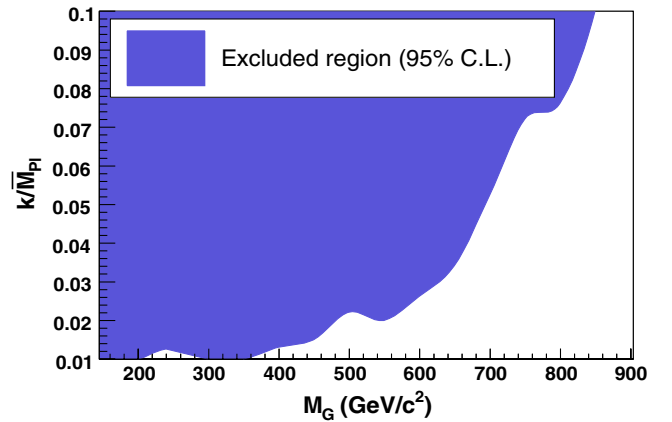

FIG. 4 (color online). $k/\bar{M}_{Pl}$ as a function of RS graviton mass. The shading indicates the region excluded at the 95% credibility level.

---

[a]Deceased.

[b]Visitor from University of Massachusetts, Amherst, Amherst, MA 01003, USA.

[c]Visitor from Universiteit Antwerpen, B-2610 Antwerp, Belgium.

[d]Visitor from University of Bristol, Bristol BS8 1TL, United Kingdom.

[e]Visitor from Chinese Academy of Sciences, Beijing 100864, China.

[f]Visitor from Istituto Nazionale di Fisica Nucleare, Sezione di Cagliari, 09042 Monserrato (Cagliari), Italy.

[g]Visitor from University of California Irvine, Irvine, CA 92697, USA.

[h]Visitor from University of California Santa Cruz, Santa Cruz, CA 95064, USA.

[i]Visitor from Cornell University, Ithaca, NY 14853, USA.

[j]Visitor from University of Cyprus, Nicosia CY-1678, Cyprus.

[k]Visitor from University College Dublin, Dublin 4, Ireland.

[l]Visitor from University of Edinburgh, Edinburgh EH9 3JZ, United Kingdom.

[m]Visitor from Universidad Iberoamericana, Mexico D.F., Mexico.

[n]Visitor from Queen Mary, University of London, London, E1 4NS, United Kingdom.

[o]Visitor from University of Manchester, Manchester M13 9PL, United Kingdom.

[p]Visitor from Nagasaki Institute of Applied Science, Nagasaki, Japan.

[q]Visitor from University of Notre Dame, Notre Dame, IN 46556, USA.

[r]Visitor from University de Oviedo, E-33007 Oviedo, Spain.

[s]Visitor from Simon Fraser University, Vancouver, British Columbia, Canada V6B 5K3.

[t]Visitor from Texas Tech University, Lubbock, TX 79409, USA.

[u]Visitor from IFIC(CSIC-Universitat de Valencia), 46071 Valencia, Spain.

[v]Visitor from University of Virginia, Charlottesville, VA 22904, USA.

[w]On leave from J. Stefan Institute, Ljubljana, Slovenia.

[1] D. London and J. L. Rosner, Phys. Rev. D **34**, 1530 (1986); F. del Aguila, M. Quiros, and F. Zwirner, Nucl. Phys. B **B287**, 419 (1987); J. L. Rosner, Phys. Rev. D **35**, 2244 (1987); J. L. Hewett and T. G. Rizzo, Phys. Rep. **183**, 193 (1989); J. Erler, P. Langacker, and T. Li, Phys. Rev. D **66**, 015002 (2002); T. Han, P. Langacker, and B. McElrath, Phys. Rev. D **70**, 115006 (2004); J. Kang and P. Langacker, Phys. Rev. D **71**, 035014 (2005).

[2] L. Randall and R. Sundrum, Phys. Rev. Lett. **83**, 3370 (1999).

[3] H. Davoudiasl, J. L. Hewett, and T. G. Rizzo, Phys. Rev. Lett. **84**, 2080 (2000); B. C. Allanach *et al.*, J. High Energy Phys. 12 (2002) 039.

[4] T. Aaltonen *et al.* (CDF Collaboration), Phys. Rev. Lett. **99**, 171802 (2007).

[5] V. Abazov *et al.* (D0 Collaboration), Phys. Rev. Lett. **100**, 091802 (2008).

[6] A. Abulencia *et al.* (CDF Collaboration), J. Phys. G **34**, 2457 (2007).

[7] We use a cylindrical coordinate system where θ is the polar angle with respect to the proton beam axis (positive z direction) and ϕ is the azimuthal angle. The pseudorapidity is $\eta = -\ln[\tan(\theta/2)]$. We define transverse energy as $E_T = E\sin\theta$ and transverse momentum as $p_T = p\sin\theta$, where E is the energy measured in the calorimeter and p is the magnitude of the momentum measured by the spectrometer.

[8] Throughout this Letter the charge conjugate state is implied.

[9] C. Issever, AIP Conf. Proc. **670**, 371 (2003).

[10] T. Sjöstrand *et al.*, Comput. Phys. Commun. **135**, 238 (2001).

[11] R. Field and R. C. Group, arXiv:hep-ph/0510198.

[12] R. Hamberg, W. L. van Neerven, and T. Matsuura, Nucl. Phys. **B359**, 343 (1991).

[13] H. L. Lai *et al.*, Phys. Rev. D **51**, 4763 (1995); J. Pumplin *et al.*, J. High Energy Phys. 07 (2002) 012.

[14] J. Pumplin *et al.*, Phys. Rev. D **65**, 014013 (2001).

[15] A. Abulencia *et al.* (CDF Collaboration), Phys. Rev. D **77**, 052002 (2008).

[16] Missing transverse energy ($\not{E}_T = |\vec{\not{E}}_T|$) is defined as $\vec{\not{E}}_T = -\sum_i E_T^i \hat{n}_i$, where $\hat{n}_i$ is a unit vector in the transverse plane that points from the beam line to the ith calorimeter tower.

[17] The $W + \gamma$ process is generated with the matrix element generator (U. Baur and E. L. Berger, Phys. Rev. D **41**, 1476 (1990)).

[18] D. Acosta *et al.*, Nucl. Instrum. Methods Phys. Res., Sect. A **494**, 57 (2002).

[19] U. Baur, T. Han, and J. Ohnemus, Phys. Rev. D **48**, 5140 (1993); J. M. Campbell and R. K. Ellis, Phys. Rev. D **60**, 113006 (1999).

[20] L. Demortier, CERN Yellow Report No. CERN-2008-001, 2008; Y. Gao, L. Lu, and X. Wang, Eur. Phys. J. C **45**, 659 (2006).

[21] σ_B is $\sqrt{N_B + \sigma_{N_B}^2}$, where N_B is the number of expected backgrounds and σ_{N_B} is the systematic uncertainty of the N_B.

[22] J. Heinrich *et al.*, arXiv:physics/0409129.

[23] C. Ciobanu *et al.*, Fermilab, Report No. FERMILAB-FN-0773-E, 2008. We note that the 2005 version of this report had a typo in the $Z'_\eta - u - u$ coupling that affected our previous publication [4].